International Journal of Mass Spectrometry 306 (2011) 138–149

Contents lists available at ScienceDirect

International Journal of Mass Spectrometry

journal homepage: www.elsevier.com/locate/ijms

A mechanistic study of the prominent loss of H_2O from ionized 2-hydroxyaminoethanol

Karl J. Jobst[a], Shaheda Jogee[b], Richard D. Bowen[b], Johan K. Terlouw[a,*]

[a] Department of Chemistry and Chemical Biology, McMaster University, 1280 Main Street West, Hamilton, Ont., Canada L8S 4M1
[b] School of Life Sciences, University of Bradford, Richmond Road, Bradford, West Yorkshire BD7 1DP UK

ARTICLE INFO

Article history:
Received 16 August 2010
Received in revised form
21 September 2010
Accepted 5 October 2010
Available online 21 October 2010

Dedicated to Professor Tino Gäumann on the occasion of his 85th birthday.

Keywords:
Tandem mass spectrometry
CBS-QB3 model chemistry
1,2-Oxazetidine
Hydrogen-bridged radical cations

ABSTRACT

Tandem mass spectrometry experiments on the HCl salt of 2-hydroxyaminoethanol reveal that low-energy ions $HOCH_2CH_2NHOH^{\bullet+}$ dissociate by loss of H_2O with remarkable efficiency (*c.* 10%). Analysis of its high energy collision-induced dissociation (CID) mass spectrum leaves little doubt that the resulting m/z 59 ion is the cyclic 1,2-oxazetidine ion, whose elusive neutral counterpart has not yet been identified by experiment.

A mechanistic analysis using the CBS-QB3 model chemistry indicates that the dissociation chemistry of $HOCH_2CH_2NHOH^{\bullet+}$ is entirely different from that of the structurally related ions $HOCH_2CH_2ONH_2^{\bullet+}$ and $HOCH_2CH_2OH^{\bullet+}$. It involves a 1,5-H transfer in one of its stable conformers that leads to a hydrogen-bridged radical cation of the 1,2-oxazetidine ion and a water molecule. In support of this proposal the isotopologues $DOCH_2CH_2NDOD{\cdot}DCl$ and $HOCH_2CD_2NHOH{\cdot}HCl$, upon ionization (almost) exclusively lose D_2O and H_2O, respectively.

1. Introduction

Some ten years ago, two unexpected disinfection by-products in chlorinated drinking water samples were tentatively identified as halogenated aminoxyalcohols [1] on the basis of various mass spectrometric experiments. This proposal was rather speculative (and as established recently, erroneous [2]) because hardly any information was available about the dissociation characteristics of ionized aminoxyalcohols. This prompted our combined experimental and theoretical study of ionized 2-aminoxyethanol, $HOCH_2CH_2ONH_2$, as a model compound [3]. Its low energy (metastable) molecular ions display a surprisingly rich chemistry involving five major dissociation pathways. The model chemistry calculations indicate that a 1,4-H shift in the molecular ion generates the ion-molecule complex $[HOCH_2(C{=}O)H^{\bullet+}]\cdots[NH_3]$, which acts as the common reacting configuration. This is in contrast to the related 1,2-ethanediol ion $HOCH_2CH_2OH^{\bullet+}$ whose dissociation chemistry is triggered by C–C bond cleavage [4]. However, proton transport catalysis (PTC) features as an important component of both mechanisms [5]. The present study deals with 2-aminoxyethanol's isomer $HOCH_2CH_2NHOH$, 2-hydroxyaminoethanol. This compound is not commercially available and all our efforts to isolate and purify it in a synthetic procedure involving the reduction of 2-nitroethanol (see Section 2) were unsuccessful. However, its (very hygroscopic) HCl salt is sufficiently stable at room temperature to be used instead for our tandem mass spectrometric measurements.

These experiments revealed that metastable ions $HOCH_2CH_2NHOH^{\bullet+}$ (**HE**-1) show a remarkably abundant (~10% of the main beam of ions) loss of H_2O to form m/z 59 ions $C_2H_5NO^{\bullet+}$ as the only reaction. Further, the labelled isotopologue $DOCH_2CH_2NDOD^{\bullet+}$ (almost) exclusively loses D_2O, whereas upon collisional activation only one important competing dissociation occurs, *viz.* the direct bond cleavage to give $^+CH_2NDOD + {}^{\bullet}CH_2OD$. Unfortunately, the structure of the product ion cannot readily be assigned on the basis of a comparison of its collision induced dissociation (CID) mass spectrum with reference spectra. A critical evaluation of the $C_2H_5NO^{\bullet+}$ system of ions has not been included in the book of [Ref. 6a] and none of the reported CID mass spectra [7,8] matches the spectrum obtained.

These intriguing and challenging observations inspired us to initiate a quest for plausible mechanisms for the H_2O elimination from metastable ions **HE**-1, using the model chemistry approach of our study of the loss of water from ionized ethyl acetate [9]. An important precondition of this approach imposed by the experimental data is that none of the stable intermediates, connecting transition states or products of a viable calculated mechanism should lie significantly higher in energy than the thermochemical threshold for direct bond cleavage to $^+CH_2NHOH$ (m/z 46) + $^{\bullet}CH_2OH$.

---

[*] Corresponding author. Tel.: +1 905 525 9140; fax: +1 905 522 2509.
E-mail address: terlouwj@mcmaster.ca (J.K. Terlouw).

1387-3806/$ – see front matter © 2010 Elsevier B.V. All rights reserved.
doi:10.1016/j.ijms.2010.10.004

Although the involvement of hydrogen-bridged radical cations (HBRCs) [10] remains a common thread, the first step of our proposed mechanism for dissociation of **HE**-1 is entirely different from that of either $HOCH_2CH_2ONH_2^{\bullet +}$ [3] or $HOCH_2CH_2OH^{\bullet +}$ [4]. It involves a unique 1,5-H transfer that leads to the formation of an ion–dipole complex comprising the four membered ring species ionized 1,2-oxazetidine [11] and a water molecule. This ion easily rearranges to a more stable HBRC but is otherwise resistant towards further isomerization and eventually loses water to yield the 1,2-oxazetidine ion (*m*/*z* 59), whose neutral counterpart is predicted to be stable by theory but it has never been characterized in the condensed phase [11].

2. Experimental and theoretical methods

2.1. Mass spectrometric measurements

The experiments were performed with the VG Analytical ZAB-R mass spectrometer of BEE geometry (B, magnet; E, electric sector) [12] using an electron ionization (EI) source at an accelerating voltage of 8 kV. Metastable ion (MI) and collision induced dissociation (CID) mass spectra were recorded in the second field free region (2ffr). The CID mass spectra of the 2ffr metastable peaks were obtained in the 3ffr using the maximum available accelerating voltage (10 kV). In all collision experiments O_2 was used as the collision gas. All spectra were recorded using a PC-based data system developed by Mommers Technologies Inc. (Ottawa). Kinetic energy releases (corrected $T_{0.5}$ values) were measured according to standard procedures [6]. The 2-hydroxyamino hydrochloride samples were introduced into the source (kept at 120 °C) via a solids probe held at ~80 °C.

Since the compound is prone to decompose and/or polymerise upon heating, the finely powdered sample was put into a 15 mm quartz probe tube into which a 17-mm gold wire was inserted to promote a better heat transfer to the sample [13]. Repeated exchange of the unlabelled hydrochloride with a five fold excess of anhydrous methanol-OD was used to prepare a sample of $DOCH_2CH_2NDOD{\cdot}DCl$. The isotopologue $HOCH_2CD_2NHOH{\cdot}HCl$ was obtained as described in the next section.

Table 1
Energetic data [a] derived from CBS-QB3 calculations of stable isomers and connecting transition states involved in the H_2O loss from 2-hydroxyaminoethanol ions **HE**-1.

Ionic species	B3LYP/CBSB7*E*(total)	CBS-QB3*E*(total) [0 K]	ZPE	QB3 $\Delta_f H^0_0$	QB3 $\Delta_f H^0_{298}$	$\langle S^2 \rangle$
HE-1a (Scheme 2)	−285.35978	−284.83556	63.5	135.4	128.9	0.77
HE-1b (Scheme 2)	−285.34046	−284.82105	62.8	144.5	138.6	0.77
HE-1c (Scheme 3)	−285.27125	−284.74447	63.3	192.6	185.9	0.76
HE-1d (Scheme 6)	−285.34622	−284.82530	63.0	141.9	135.7	0.77
HE-2 (Scheme 3)	−285.31495	−284.79097	62.9	163.4	157.5	0.77
HE-3 (Scheme 3)	−285.32520	−284.81197	60.8	150.2	145.2	0.77
HE-4 (Scheme 6)	−285.29201	−284.77017	62.3	176.5	170.1	0.76
HE-5a (Scheme 6)	−285.30766	−284.78676	62.7	166.0	160.3	0.76
HE-5b (Scheme 6)	−285.30814	−284.78634	62.8	166.3	160.4	0.76
HE-6 (Scheme 6)	−285.31428	−284.79130	63.6	163.2	156.8	0.76
HE-7 (Scheme 6)	−285.33672	−284.81645	63.4	147.4	141.6	0.76
HE-8 (Scheme 6)	−285.36753	−284.83922	61.3	133.1	127.4	0.87
HBRC-2 (Scheme 2)	−285.31604	−284.79503	60.5	160.8	155.7	0.77
HBRC-3a (Scheme 3)	−285.34062	−284.82301	61.0	143.3	137.8	0.77
HBRC-3b (text)	−285.30697	−284.78556	58.3	166.8	161.8	1.13
HBRC-3c (text)	−285.26569	−284.74042	57.8	195.1	190.4	0.99
HBRC-4a (Scheme 3)	−285.39141	−284.86930	60.6	114.2	109.0	0.76
HBRC-4b (Scheme 3)	−285.30393	−284.78940	60.7	164.4	159.0	0.76
HBRC-5 (Scheme 6)	−285.32809	−284.80603	60.8	153.9	148.2	0.77
HBRC-6 (Scheme 6)	−285.30847	−284.79012	59.6	163.9	158.1	0.76
HBRC-7 (Scheme 6)	−285.37620	−284.85243	60.8	124.8	119.5	0.94
TBC-1a (Scheme 2)	−285.34977	−284.82238	58.3	143.7	139.1	0.90
TBC-1b (Scheme 2)	−285.37368	−284.85626	56.2	122.4	118.2	0.90
TBC-2 (Scheme 2)	−285.35603	−284.84186	56.2	131.5	127.2	0.89
TS **HE**-1a → b	−285.33319	−284.80938	62.1	151.8	145.4	0.77
TS **HE**-1a → d	−285.32657	−284.80329	61.6	155.7	149.6	0.77
TS **HE**-1a → 4	−285.28650	−284.76499	60.3	179.7	172.9	0.77
TS **HE**-1d → 6	−285.29041	−284.76705	59.6	178.4	171.7	0.76
TS **HE**-1a → 7	−285.28343	−284.76208	60.2	181.5	175.1	0.80
TS **HE**-1d → 5a	−285.30618	−284.78445	62.6	167.5	161.1	0.76
TS **HE**-1a → 2	−285.31237	−284.78854	63.0	164.9	158.4	0.77
TS **HE**-1a → **HBRC**-2a	−285.31077	−284.78824	60.8	165.1	159.2	0.81
TS **HE**-1b → **TBC**-1a	−285.29602	−284.77247	58.3	175.0	169.4	0.78
TS **HE**-1a → **HBRC**-7	−285.28034	−284.75959	59.3	183.1	176.8	0.77
TS **HE**-2 → 3	−285.30661	−284.78320	61.1	168.3	162.6	0.77
TS **HE**-3 → **HBRC**-3a	−285.32392	−284.80972	60.8	151.6	146.0	0.77
TS **HE**-3 → **HBRC**-3c	−285.30027	−284.78463	58.0	167.4	162.2	0.76
TS **HE**-3 → **HBRC**-4b	−285.26048	−284.74542	59.6	192.0	186.0	0.76
TS **HE**-4 → **MF**4	−285.28889	−284.76517	60.7	179.6	173.5	0.76
TS **HE**-5a → 5b	−285.30711	−284.78546	62.6	166.9	160.5	0.76
TS **HE**-5a → **HBRC**-5	−285.29363	−284.77261	60.1	174.9	169.3	0.78
TS **HE**-5b → **HBRC**-6	−285.27585	−284.75750	59.9	184.4	178.7	0.76
TS **HBRC**-4b → a	−285.28454	−284.77067	59.9	176.1	170.4	1.20
TS **HBRC**-6 → 3a	−285.29607	−284.78075	60.8	169.8	164.0	0.77
TS **TBC**-1a → 1b	−285.33691	−284.81986	55.9	145.3	141.0	0.87

[a] *E*(total) in Hartrees, all other components, including the ZPE scaled by 0.99, are in kcal mol^{-1}.

2.2. Synthesis of 2-hydroxyaminoethanol and its isotopologue $HOCH_2CD_2NHOH$

Although the reduction of simple nitrocompounds to the corresponding amines may be accomplished by a wide variety of means without difficulty, the partial reduction to form hydroxylamines is far less straightforward. Substituted hydroxylamines are much less stable than either the starting nitrocompounds or the analogous amines; moreover, it is often difficult to prevent over-reduction to the amine. Some of these problems may be overcome, at least in principle, by generating and isolating the salts of the free bases, which are less prone to decomposition; however, these salts are frequently extremely hygroscopic, particularly when the substituent contains a hydroxyl or related hydrophilic group. Isolation of 2-hydroxyaminoethanol as the free base ($HOCH_2CH_2NHOH$) was found to be impractical, but its hydrochloride could be generated in situ during the reaction work up, isolated as a hygroscopic solid and subjected to mass spectrometry.

Several methods may be found in the literature for the reduction of nitroalcohols to hydroxyaminoalcohols (and their salts). The two main ways are by means of catalytic hydrogenation (usually under high initial pressure and with partially poisoned catalysts [14a]) and the use of dissolving metals (typically zinc [14b] or amalgams containing aluminium or sodium [14c]). Other methods include the use of the cyanohydridoborate anion [14d] and diborane [14c]; more recently, samarium di-iodide under anhydrous conditions has been found to be effective [14e]. Many of these published procedures either lack experimental detail, require highly specialised apparatus (such as high pressure hydrogenation equipment) or conditions (rigorous exclusion of water and/or the use of expensive and highly sensitive reagents) and special precautions to deal with the toxicity of the reagents or by-products. The most promising method of reducing $HOCH_2CH_2NO_2$ to $HOCH_2CH_2NHOH$ and converting it to $HOCH_2CH_2NHOH{\cdot}HCl$ appeared to be to use purified zinc dust in the presence of aqueous methanol containing NH_4Cl [14b]. Even in this case, however, it proved impossible to repeat the synthesis from the information available in the literature. The following modified procedure was eventually devised after preliminary experiments with the homologue, 2-nitropropanol.

A solution of 2-nitroethanol (3.33 g, 37 mmol) and NH_4Cl (5.35 g, 100 mmol) dissolved in aqueous methanol (25 ml, 80%, v/v water) was stirred vigorously while purified zinc powder (4.91 g, 75 mmol, washed with dilute HCl, water and acetone, and dried to constant mass) was added in small portions during 10 min. The rate of addition was controlled so that the temperature gradually rose to 60–65 °C; this temperature was maintained until all the zinc had been added, whereupon it began to fall. The mixture was stirred for a further 15 min. The warm residue was filtered at the pump and the inorganic salts were extracted on the filter with aqueous methanol (70 ml, 80%, v/v water). The excess methanol was removed from the combined filtrate and extracts by rotary evaporation (warm water bath) to leave a yellow liquid, which was carefully washed with diethyl ether (3 ml × 15 ml) to remove any remaining starting material. Excess HCl in methanol (50 ml, containing a minor amount of methyl acetate) was added and the liquid was rotary evaporated to constant mass (in a water bath whose temperature was progressively raised to 90 °C) to remove the methyl acetate, methanol and water. The residual amber hygroscopic solid (6.17 g, 82%) was analysed by ^1H NMR in D_2O; the organic component (comprising some 56% of the total mass, as established by adding a known quantity of starting material to an aliquot of product and comparing the integrations of relevant signals) appeared to consist essentially entirely of the desired product, $HOCH_2CH_2NHOH{\cdot}HCl$. ^1H NMR [400 MHz, in D_2O: δ 3.35, 2H, *t* (J = 5.2 Hz) and 3.86, 2H, *t* (J = 5.2 Hz)].

As mentioned above, the HCl salt was found not to undergo smooth and sustained dissociation and evaporation from the probe, even when a method devised for introduction of salts was employed. Therefore, the corresponding CH_3COOH and CF_3COOH salts were prepared by modifying the method used to make the HCl salt. Unfortunately, however, these salts were only marginally easier to analyse by mass spectrometry than the HCl salt.

The following procedure was devised to prepare $HOCH_2CD_2NO_2$ for reduction to $HOCH_2CD_2NHOH{\cdot}HCl$. A solution of 2-nitroethanol (6.0 g, 66 mmol) and dry K_2CO_3 (0.54 g, 4 mmol) in D_2O (20 ml, 22.1 g, 1 mol) was stirred magnetically under an N_2 atmosphere at ambient temperature. The exchange of the protons α- to the nitro group was monitored by ^1H NMR by following the decrease in intensity of the signal at δ 4.52 and the collapse of the triplet signal at δ 4.10 to a singlet. The level of D-incorporation at the 2-position reached the theoretical limit of ~90% after approximately

Table 2
Energetic data derived from CBS-QB3 calculations [a] used to probe the dissociation chemistry of ionized 2-hydroxyaminoethanol.

Species and mass		CBS-QB3 E(total) [0 K]	QB3 $\Delta_fH^0{}_{298}$
Fig. 1 ion **1**a	59	−208.48964	195.1
Fig. 1 ion **1**b	59	−208.46601	210.0
Fig. 1 ion **1**c	59	−208.46966	207.5
Fig. 1 ion **1**d	59	−208.49580	189.9
Fig. 1 ion **2**a	59	−208.48141	200.2
Fig. 1 ion **2**b	59	−208.48213	198.8
Fig. 1 ion **3**a	59	−208.45631	214.6
Fig. 1 ion **3**b	59	−208.43716	227.0
Fig. 1 ion **3**c	59	−208.41518	240.8
Fig. 1 ion **3**d	59	−208.37704	264.6
Fig. 1 ion **4**a	59	−208.50553	183.8
Fig. 1 ion **4**b	59	−208.42220	235.9
Fig. 1 ion **5**	59	−208.43420	228.4
Fig. 1 ion **6**	59	−208.40726	245.2
Fig. 1 ion **7**	59	−208.48277	198.5
Fig. 1 ion **8**	59	−208.48568	196.6
Fig. 1 ion **9**	59	−208.41263	242.3
$CH_2{=}O$	30	−114.34417	−27.0
$CH_2OH^{\bullet}$	29	−114.88817	−5.2
$CH_3O^{\bullet}$	29	−114.87541	3.9
$CH_2{=}NH^{\bullet+}$	29	−94.10039	250.7
$H{-}C{-}NH_2{}^{\bullet+}$	29	−194.10578	247.2
$HC{\equiv}NH^+$	28	−93.55430	226.4
$CH_2{=}N^{\bullet}$	28	−93.82791	57.2
H_2O	18	−76.33750	−57.0
Fig. 1 ion **10**	59	−208.45234	217.7
Fig. 1 ion **11**	59	−208.45250	217.5
Fig. 1 ion **12**	59	−208.56543	146.2
Fig. 1 ion **13**	59	−208.50780	179.0
TS **3**a → **3**b		−208.39717	251.5
TS **3**b → **9**		−208.39550	252.7
TS **9** → m/z 28		−208.40230	249.1
TS **3**b → **1**c		−208.42975	231.7
TS **1**c → **1**d		−208.45341	217.1
TS **1**d → **2**b		−208.44142	223.8
Fig. 1 ion MF-1	59	−208.51247	179.8
Fig. 1 ion MF-2	59	−208.50594	184.3
Fig. 1 ion MF-3	59	−208.51584	177.8
Fig. 1 ion MF-4	59	−208.54478	159.2
Fig. 1 neutral DP-1	58	−208.10729	69.1
Fig. 1 neutral DP-2	58	−208.17041	29.9
Fig. 1 neutral DP-3	58	−208.17183	28.9
$CH_2{=}O{\cdots}H{\cdots}OH_2{}^+$	49	−190.99545	81.5
$CH_2{=}N{\cdots}H{\cdots}OH_2{}^{\bullet+}$	47	−170.48072	165.1
$CH_2{=}N(H){\cdots}OH_2{}^{\bullet+}$	47	−170.45287	182.4
$CH_2{=}NHOH^+$	46	−169.87875	177.3
$CH_2{-}CH_2{-}OH_2{}^{\bullet+}$	45	−154.39990	176.8
$CH_2{=}C{=}NH^{\bullet+}$	41	−132.16308	247.0
HNO	31	−130.32328	24.8

[a] E(total) in Hartrees, 298 K enthalpies in kcal mol^{-1}. Numbers for ions AA1–4 in Fig. 1 are from Ref. [8].

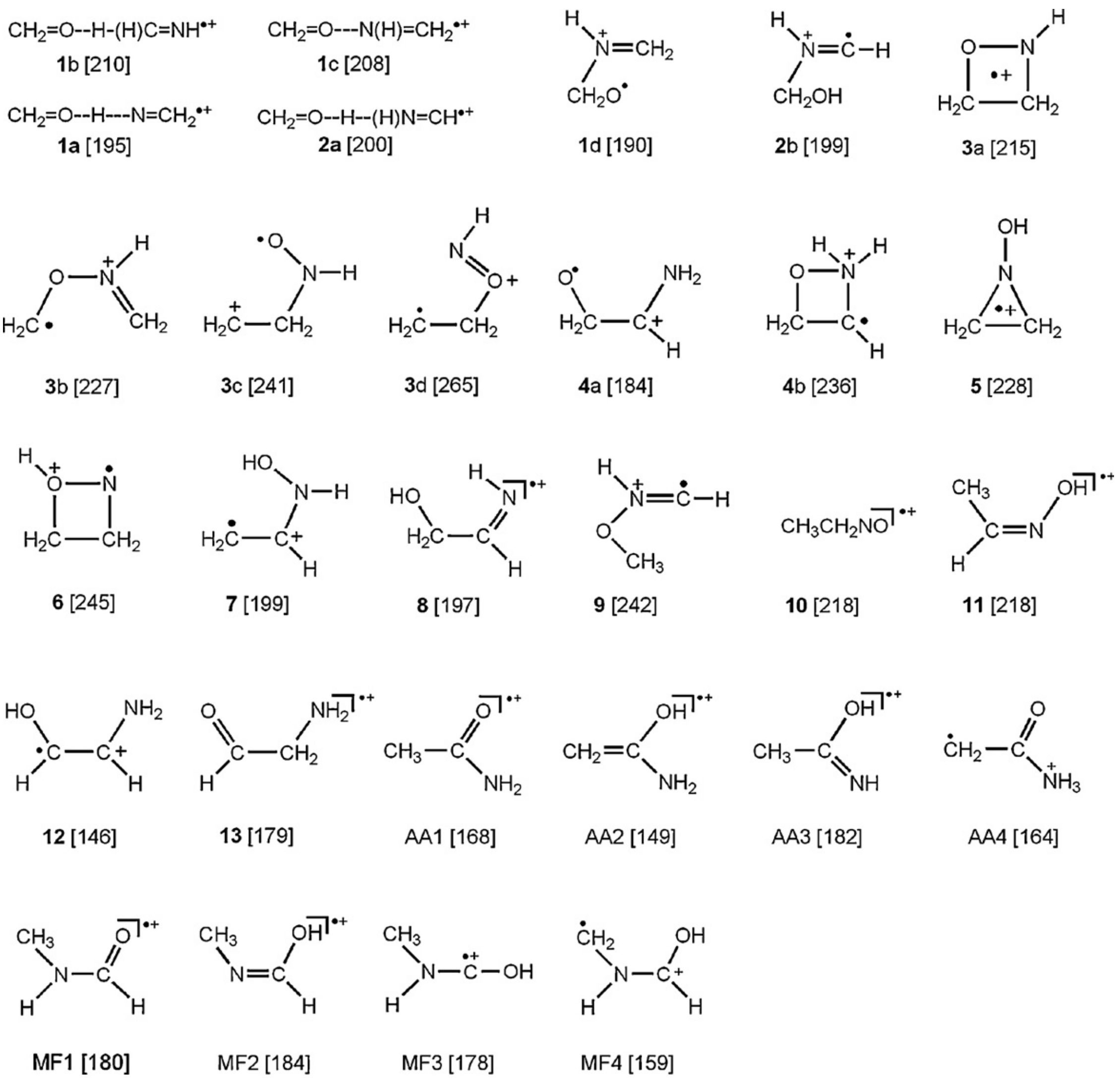

Fig. 1. Structures of m/z 59 C_2H_5NO product ions and their enthalpies of formation (298 K values in kcal mol^{-1} derived from CBS-QB3 calculations, see Table 2).

36 h. The mixture was saturated with salt and the partially labelled 2-nitroethanol was isolated by extraction with CH_2Cl_2 (5×20 ml); the combined extracts were dried (with $MgSO_4$), filtered and evaporated at reduced pressure to give a yellow liquid (4.8 g, 78%). This material was then subjected to another exchange with a second portion of D_2O (20 ml, 1 mol) and fresh K_2CO_3 (0.40 g, 3 mmol) to give $HOCH_2CD_2NO_2$ (3.4 g, 71%) with *c.* 97% D-incorporation at the 2-position.

The labelled 2-nitroethanol was reduced as described above for the unlabelled analogue to give $HOCH_2CD_2NHOH{\cdot}HCl$ as a yellow solid, from which the desired $HOCH_2CD_2NHOH^{\bullet+}$ isotopologue could be generated.

2.3. Theoretical calculations

The calculations were performed with the CBS-QB3 model chemistry [15]; for selected species the (computationally much more demanding) CBS-APNO method [16] was also used. Most of the calculations were run with the Gaussian 2009, Rev A.02 suite of programs [17] on the SHARCNET computer network at McMaster University. In the CBS-QB3 model chemistry the geometries of minima and connecting transition states are obtained from B3LYP density functional theory in combination with the 6-311G(2d,p) basis set (also denoted as the CBSB7 basis set). The resulting total energies and enthalpies of formation for minima and connecting transition states (TS) in the 2-hydroxyaminoethanol system of ions are presented in Table 1. Computational data pertaining to the dissociation products are found in Table 2. Spin contaminations ($\langle S^2 \rangle$ values of Table 1) were acceptable. Optimized geometries (B3LYP/CBSB7) of selected minima and transition states are shown in Fig. 5. Unless stated otherwise, all enthalpies presented in the text and in the schemes (numbers in square brackets) refer to $\Delta_f H^o{}_{298}$ values in kcal mol^{-1} derived from the CBS-QB3 calculations. The complete set of computational results is available from the authors upon request.

3. Results and discussion

3.1. Identification of the m/z 59 ions generated from metastable ions $HOCH_2CH_2NHOH^{\bullet+}$

Before considering various mechanistic proposals for the water loss from metastable ions $HOCH_2CH_2NHOH^{\bullet+}$, we will first focus on the structure assignment of the $C_2H_5NO^{\bullet+}$ product ion. In lieu of a critical review [6a] of this system of ions, we have compiled the selection of isomers shown in Fig. 1 with their computed enthalpies of formation. As pointed out in Section 1, the energy required for the water loss must not exceed that

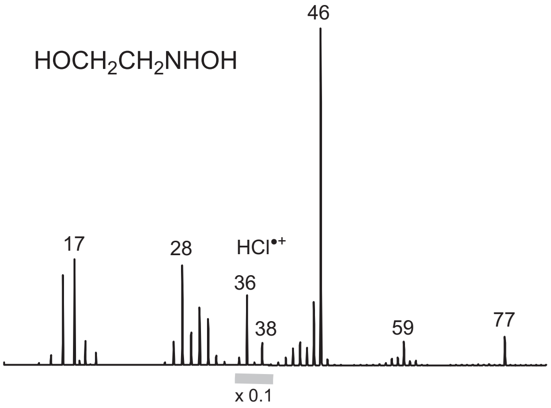

Fig. 2. 70 eV EI mass spectrum of 2-hydroxyaminoethanol hydrochloride.

for the direct bond cleavage to CH_2NHOH^+ (*m*/*z* 46) + $CH_2OH^\bullet$ ($\Sigma\Delta_fH^{298} = 171\ \text{kcal mol}^{-1}$), which is an important reaction in the EI and CID mass spectra shown in Figs. 2 and 3b. This criterion dictates that $\Delta_fH^{298}(C_2H_5NO^{\bullet+}) + \Delta_fH^{298}(H_2O) \leq 171\ \text{kcal mol}^{-1}$, or an upper limit of $229\ \text{kcal mol}^{-1}$ for the enthalpy of formation of the $C_2H_5NO^{\bullet+}$ ions that comprise the single intense peak at *m*/*z* 59 in the MI mass spectrum of Fig. 3a.

The previously studied ions **MF**1–4 and **AA**1–4 of Fig. 1 satisfy this criterion, but the prominent structure diagnostic peaks of their CID mass spectra [7,8] are not compatible with the spectrum of Fig. 3c: ions **AA**1–4 predominantly lose NH_3, $NH_2^\bullet$ and $CH_3^\bullet$ to generate ions of *m*/*z* 42–44, whereas ions **MF**1, **MF**2 and **MF**3 produce intense peaks at *m*/*z* 30, 42 and 44 for loss of $HCO^\bullet$, $OH^\bullet$ and $CH_3^\bullet$, respectively. The CID mass spectrum of the distonic ion **MF**4 resembles that of **MF**1 but it displays a unique intense charge stripping peak at *m*/*z* 29.5. In this context we note that ions **10–13** of Fig. 1 (whose CID mass spectra are not available from the literature) are unlikely candidates as well. Simple thermochemical considerations lead to the expectation that ions **10** and **11** will show a prominent loss of $CH_3^\bullet$ upon collisional activation. Acetaldoxime ions **11** may also readily lose H_2O as witnessed by the prominent *m*/*z* 41 peak in its reported EI mass spectrum [6d] and this may also be true for the enol ion **12**, which probably represents the global minimum of the $C_2H_5NO^{\bullet+}$ system of ions. Alternatively, ion **12** may rearrange into its 1,3-H shift isomer **13**, $H_2NCH_2C(H){=}O^{\bullet+}$, and then readily dissociate into $CH_2NH_2^+$ (*m*/*z* 30) + $HCO^\bullet$, rather than HCO^+ (*m*/*z* 29) + $CH_2NH_2^\bullet$, which requires ~45 kcal mol^{-1} more energy [6a,c].

The CID mass spectrum of Fig. 3c displays a prominent pair of ill resolved broad peaks at *m*/*z* 29 and *m*/*z* 28. These peaks likely represent ions $CH_3N^{\bullet+}$ ($CH_2{=}NH^{\bullet+}$ or $HCNH_2^{\bullet+}$ [6a]) and CH_2N^+ ($HC{\equiv}NH^+$), rather than $C_2H_5^+/C_2H_4^{\bullet+}$. In line with this proposal, the *m*/*z* 29 peak shifts to *m*/*z* 30 in the CID mass spectrum of the $C_2H_4DNO^{\bullet+}$ ions, see Fig. 3d, generated from the isotopologue $DOCH_2CH_2NDOD^{\bullet+}$. Since the D_2O loss is (almost) specific, it is a sound assumption that the methylene hydrogens do not readily exchange with the D-atoms by unimolecular processes. Thus, it is impossible that a D-atom would become incorporated at a carbon atom in $C_2H_5^+$. We further note that the large width of the peaks ($T_{0.5}$ is ~600 meV) indicates that the dissociation of the *m*/*z* 59 ions to *m*/*z* 29 and *m*/*z* 28 ions is associated with a substantial reverse energy barrier.

Another feature of Fig. 3c is the cluster of unresolved peaks at *m*/*z* 24–27, corresponding to ions $C_2^{\bullet+}$, C_2H^+, $C_2H_2^{\bullet+}$ and $C_2H_3^+$, which attests to the C–C atom connectivity of the $C_2H_5NO^{\bullet+}$ ions. Confirmation of this deduction is found in the observation that these peaks do not shift in the CID spectrum of Fig. 3d.

In summary, the structure of the $C_2H_5NO^{\bullet+}$ ion must have the following characteristics: (i) its heat of formation (Δ_fH^{298}) must

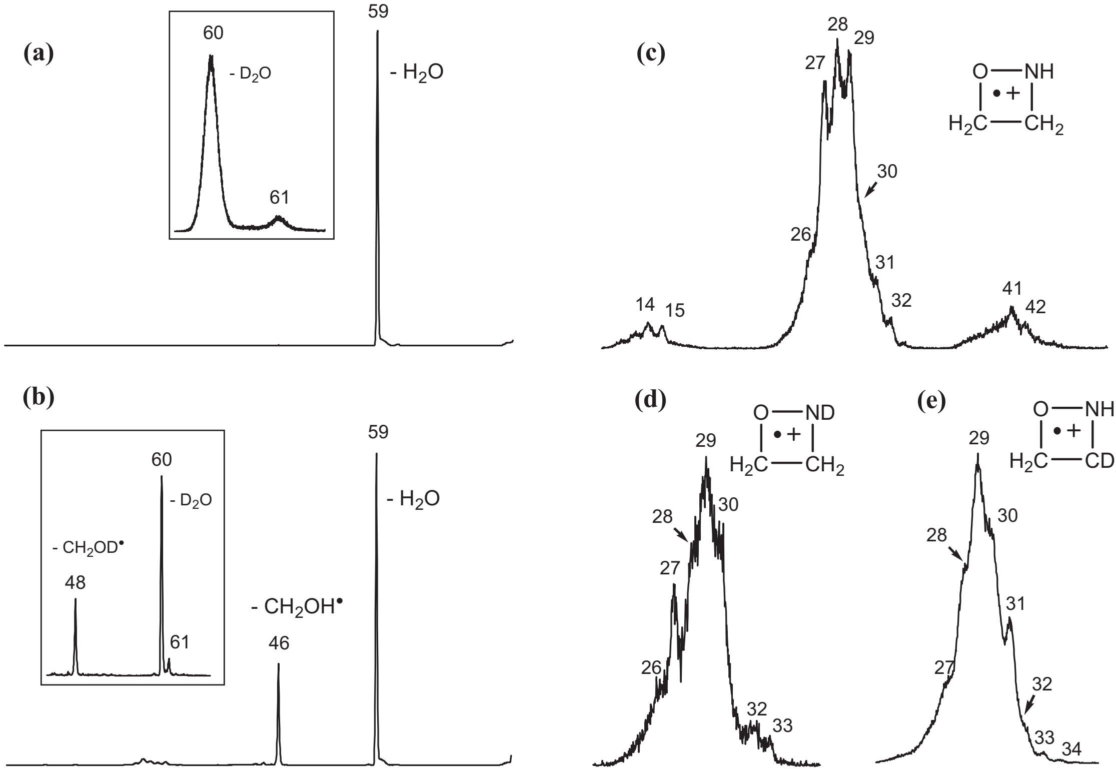

Fig. 3. MI and CID spectra of molecular ions $HOCH_2CH_2NHOH^{\bullet+}$, items (a) and (b) respectively. The insets refer to the corresponding spectra of the isotopologue $DOCH_2CH_2NDOD^{\bullet+}$. Item (c) is the CID spectrum of the *m*/*z* 59 ions generated from metastable ions $HOCH_2CH_2NHOH^{\bullet+}$ while items (d) and (e) represent the corresponding partial spectra of the *m*/*z* 60 and 61 ions from $DOCH_2CH_2NDOD^{\bullet+}$ and $HOCH_2CD_2NHOH^{\bullet+}$, respectively. Spectra (c) and (d) contain a partially resolved peak for loss of $H^\bullet$ with an intensity of ~30% of the base peak.

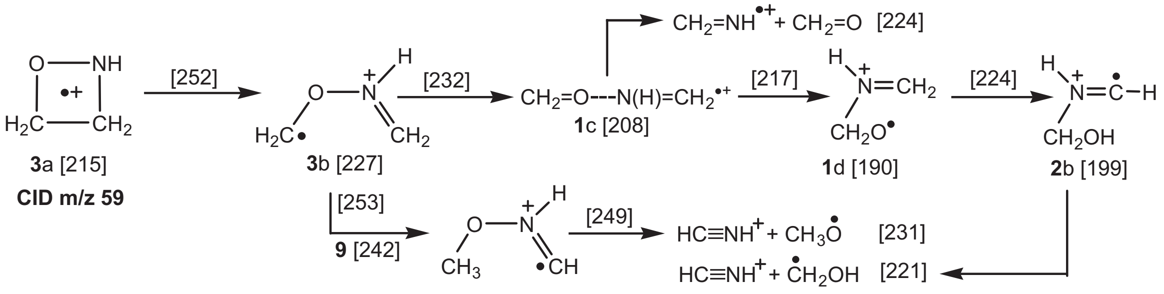

Scheme 1.

not exceed 229 kcal mol^{-1}; (ii) the ion must have a structure motif (CH_2=NH or H–C–NH_2) that accounts for the generation of *m*/*z* 29 and *m*/*z* 28 ions upon collisional activation with a substantial kinetic energy release; (iii) the ion has a C–C atom connectivity.

Based on these characteristics, only ions **3**a, **4**a, **7** and **8** of Fig. 1 retain their candidacy as potential product ions. However, it is unlikely that we are dealing with ions **7** or **8**, considering that their CID mass spectra are expected to show a significant *m*/*z* 41 peak for loss of H_2O: in these ions, the thermochemically favourable generation of CH_2=C=$NH^{\bullet+}$ + H_2O ($\Sigma\Delta H_f$ = 189 kcal mol^{-1}) can be realized by a simple 1,3-H shift.

To decide between the remaining possibilities, namely the cyclic ion **3**a and the distonic ion **4**a, we have explored their dissociation characteristics. Theory indicates that ring-opening of ion **3**a to **3**b requires less energy than that to **3**c or **3**d, see Fig. 1, but even the C–C bond cleavage is associated with a substantial reverse barrier. As shown above (Scheme 1), the computed dissociation sequence **3**a → **3**b → **1**c → CH_2=$NH^{\bullet+}$ (*m*/*z* 29) and the competing rearrangements **3**b → **1**c → **1**d → **2**b → HC≡NH^+ (*m*/*z* 28) and **3**b → **9** → HC≡NH^+ (*m*/*z* 28) may account for the pair of broad peaks at *m*/*z* 29 and *m*/*z* 28 in the CID mass spectrum of Fig. 3c.

In contrast, theory predicts that the dissociation **4**a → H–C–$NH_2^{\bullet+}$ (*m*/*z* 29) + CH_2=O is a barrierless reaction, which does not account for the experimental observations. In addition, a simple 1,4-H shift in ion **4**a would produce ion **8** and lead, as argued above, to a significant loss of water, which is not observed.

Thus we propose that the CID mass spectrum of Fig. 3c represents the cyclic ion **3**a, ionized 1,2-oxazetidine, whose elusive neutral counterpart has not (yet) been identified by experiment [11].

3.2. Does the loss of H_2O from $HOCH_2CH_2NHOH^{\bullet+}$ involve cleavage of the C–C bond?

In our mechanistic analysis of the water loss from ionized 2-hydroxyaminethanol (**HE**1), we will first consider the selection of conformers **HE**1a–e and their neutral counterparts **HE**N1a–e shown in Fig. 4.

Surprisingly, the most stable ionic conformer, **HE**1a, is not the most stable neutral conformer: the internally hydrogen bridged conformer **HE**N1c is more stable by 1.6 kcal mol^{-1}. However, ionization of **HE**N1c does not yield a minimum while its related 1,5-H shift isomer **HE**1c lies an astounding 57 kcal mol^{-1} higher in energy than **HE**1a. A plausible explanation for these remarkable results is that ionization takes place at the hydroxylamine moiety: the localized positive charge would repel the bridging hydrogen and thus raise the energy. Indeed, a charge distribution analysis supports this view and the transformation of the N-pyramidal geometry of neutrals **HE**N1a–e into the planar geometry of ions **HE**1a–e indicates the removal of a nitrogen lone pair electron (Fig. 5).

The difference in the geometries of the ions and neutrals is also borne out by the substantial difference in vertical and adiabatic ionization energies: the calculations predict that vertical ionization of neutrals **HE**N1a–e, as normally occurs during EI, would yield excited ions at 158, 166, 172, 167 and 164 kcal mol^{-1}.

As becomes clear from Scheme 2, ions generated from **HE**N1c have sufficient energy to dissociate to CH_2NHOH^+ (*m*/*z* 46) + $CH_2OH^\bullet$, which may well explain the moderate intensity of the *m*/*z* 77 molecular ion relative to the *m*/*z* 46 peak in the EI mass spectrum of Fig. 2. On the other hand, neutrals **HE**N1a, 1b, 1d and 1e yield ions with onset energies that are quite high but insufficient to promote dissociation to the *m*/*z* 46 ion. This result is consistent

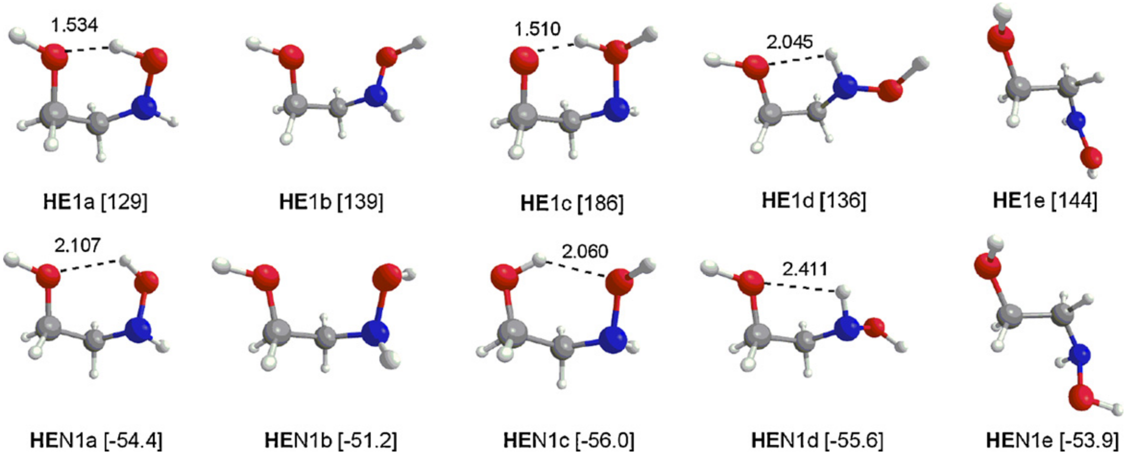

Fig. 4. Optimized geometries of various conformers of ionized 2-hydroxyaminoethanol (**HE**1a–e) and their neutral counterparts (**HE**N1a–e).

with the remarkably high population of metastable ions, as witnessed by the *c.* 10% abundance of the *m*/*z* 59 peak for loss of H_2O relative to the main beam in the MI mass spectrum. Interestingly, the metastable ions can still undergo C–C bond cleavage, albeit to generate the stable hydrogen-bridged radical cation **HBRC**2 of Scheme 2. Although the formation of **HBRC**2 appears to be a *cul-de-sac* rearrangement, these findings raise the intriguing question of whether another C–C bond cleavage initiates the loss of water from metastable ions **HE**1.

Scheme 2 indicates that ion **HE**1a readily interconverts with its conformer **HE**1b via a rotational TS at 145 kcal mol^{-1}. The next step involves an energy demanding transfer of the hydroxylic hydrogen to the hydroxylamine group in concert with cleavage of the C–C bond. The resulting ion, **HBRC**1, is not a minimum and rearranges to a ter-body complex [18], ion **TBC**1a, by elongation of the N–O bond. The long N–O bond (2.16 Å) is characteristic of a two-center three electron bond [19]. Loss of H_2O from **TBC**1a would yield the stable hydrogen-bridged radical cation ion **1**a as the *m*/*z* 59 product ion. However, theory predicts that **TBC**1a smoothly rearranges to the remarkably stable isomer **TBC**1b. These ions may subsequently generate *m*/*z* 47 and 49 ions with the same energy requirement as that for the loss of water. Signals at *m*/*z* 47 or 49 are not detectable in the MI mass spectrum of **HE**1, so we conclude that the water loss is not initiated by C–C bond cleavage.

3.3. The proposed mechanism for the loss of H_2O from metastable ions $HOCH_2CH_2NHOH^{\bullet +}$

As shown in the previous section, ion **HE**1a is the most stable conformer of ionized 2-hydroxyaminoethanol because of the favourable O–H–O interaction. Cleavage of the C–C bond of **HE**1a, while preserving the integrity of the hydrogen bridge, yields the remarkably stable ion **HBRC**2. In this section, we will show that the key step in the water loss mechanism involves transfer of the bridging hydrogen of **HE**1a while the integrity of the C–C bond is preserved.

Scheme 3 indicates that the isomerization **HE**1a → **HE**2 is a continuously endothermic process involving transfer of the bridging hydrogen in concert with rotation of the C–C bond. Ion **HE**2 is a reasonably stable species, which lies at 158 kcal mol^{-1} and needs only 5 kcal mol^{-1} of internal energy to ring-close to the ion–dipole complex **HE**3 (IDC). Subsequent loss of water from **HE**3 yields the cyclic species **3**a, ionized 1,2-oxazetidine. The calculations also show that **HE**3 readily isomerizes into the more stable hydrogen-bridged radical cation **HBRC**3a.

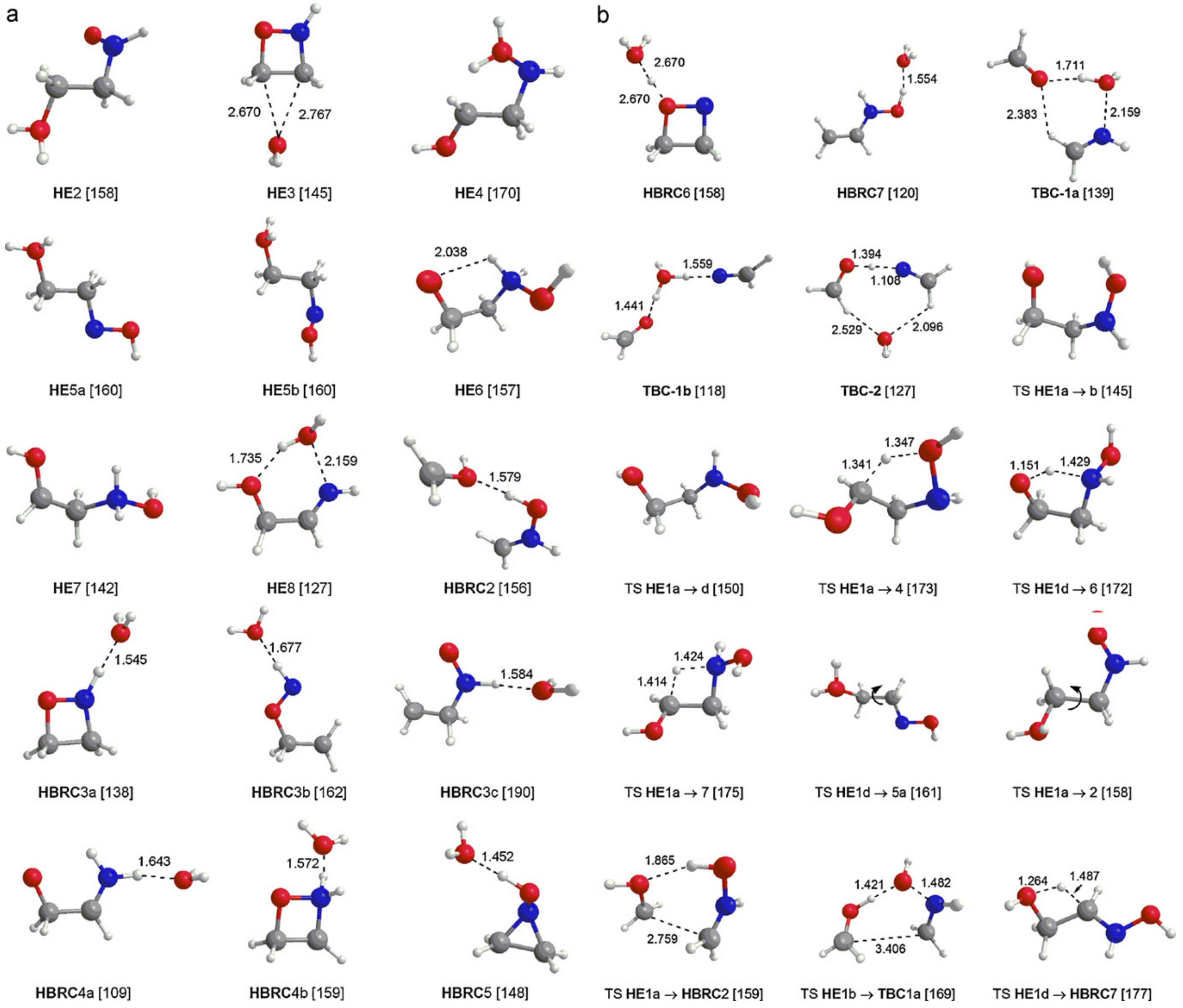

Fig. 5. Optimized geometries (B3LYP/CBSB7) of minima and transition states involved in the water loss from ionized 2-hydroxy-aminoethanol (**HE**-1).

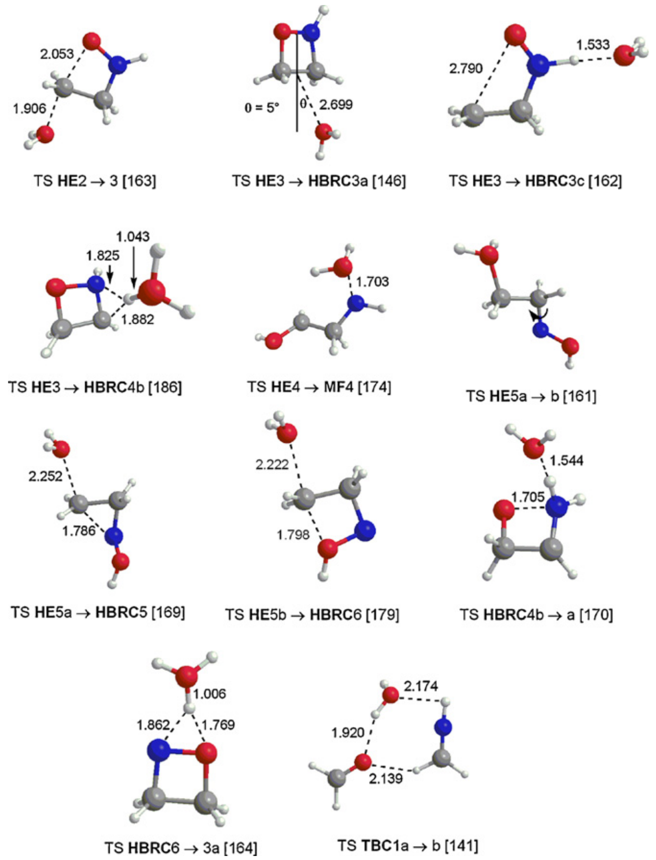

TS **HE2** → 3 [163]

TS **HE3** → **HBRC3a** [146]

TS **HE3** → **HBRC3c** [162]

TS **HE3** → **HBRC4b** [186]

TS **HE4** → **MF4** [174]

TS **HE5a** → b [161]

TS **HE5a** → **HBRC5** [169]

TS **HE5b** → **HBRC6** [179]

TS **HBRC4b** → a [170]

TS **HBRC6** → 3a [164]

TS **TBC1a** → b [141]

Fig. 5. (*Continued*).

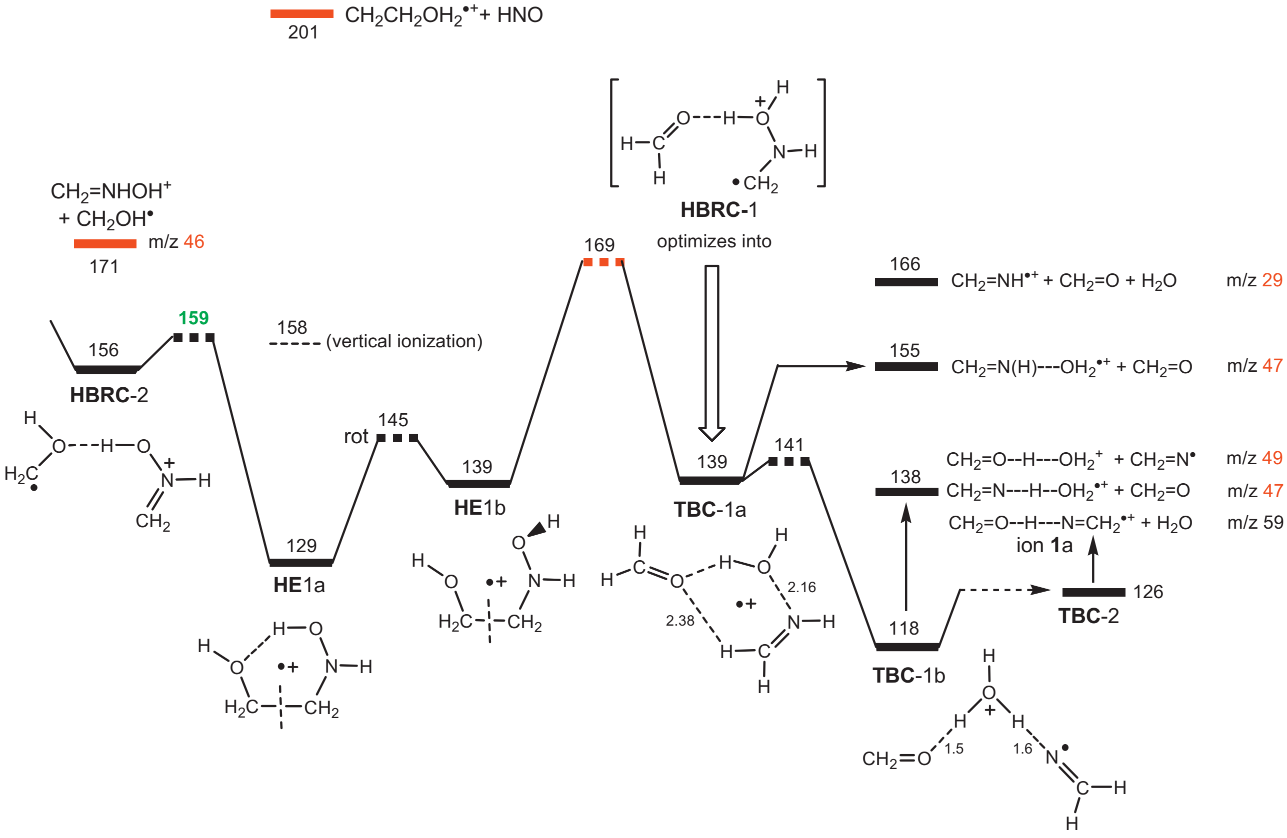

Scheme 2.

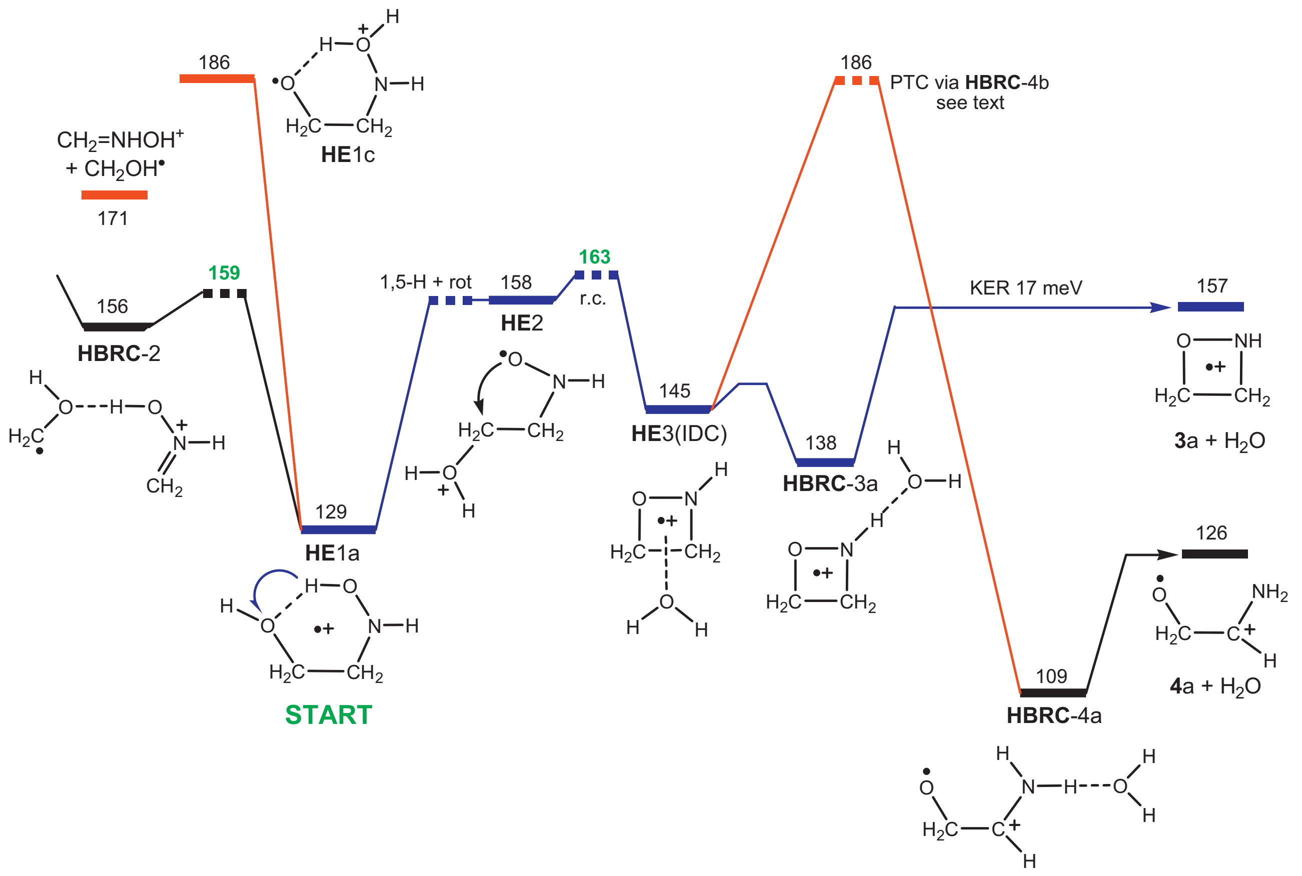

Scheme 3.

The significant stabilization enjoyed by **HBRC**3a with respect to water loss raises the intriguing question of whether further isomerization within the ion-molecule complex takes place. Scheme 4 indicates that fission of the C–C and C–N bonds is too energy demanding, but that the TS for ring-opening to **HBRC**3c lies slightly below the critical energy of the reaction **HE**1a → **HBRC**3a. This implies that a small fraction of the metastable **HE**1 ions could communicate with ions **HBRC**3c, but the reaction is circuitous because of the high energy required for their subsequent dissociation to **3**c + H_2O.

Another interesting question is whether the water molecule of **HE**3 catalyzes the isomerization of **3**a to the energy rich ion **4**a by a process termed proton-transport catalysis (PTC) [5]. The proposed two-step reaction mechanism is depicted in Scheme 5.

The first step involving PTC requires that the water molecule abstracts a methylene proton from **HE**3 and transfers it to the nitrogen to generate **HBRC**4b. In the second step, **HBRC**4b ring-opens to **HBRC**4a. However, theory predicts that the PTC reaction does not occur because the associated TS lies 29 kcal mol^{-1} above the dissociation threshold **3**a + H_2O. This result is not surprising considering the fact that the proton affinity of H_2O (165 kcal mol^{-1}) is considerably lower than that required to abstract the methylene proton (220 kcal mol^{-1}). These findings leave little doubt that incipient ions **HE**3 and **HBRC**3a have no alternative but to dissociate into **3**a + H_2O.

Thus, the mechanistic proposal of Scheme 3 agrees well with the experimental findings discussed in Section 3.1 in terms of the structure of the $C_2H_5NO^+$ ions and the energy requirement of the reaction. The reverse barrier of the dissociation (6 kcal mol^{-1}, Scheme 3) is associated with a kinetic energy release (KER) of only 0.5 kcal mol^{-1} (17 meV). If a covalent bond were cleaved, the KER would be expected to be significantly larger. However, as with the celebrated case of the H_2O loss from metastable n-propanol ions [4], the precursor to dissociation (**HE**3) is an ion–dipole complex and

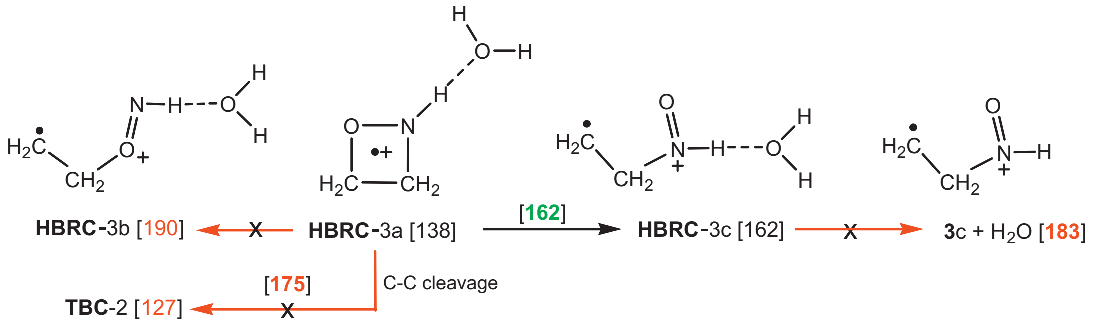

Scheme 4.

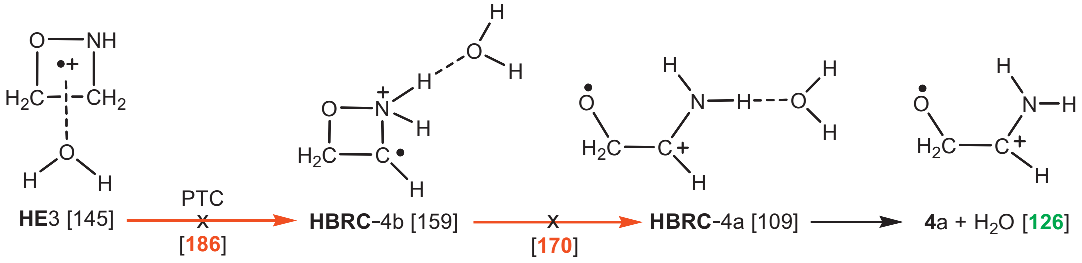

Scheme 5.

for such ions only a minor fraction of the excess internal energy is partitioned among translational degrees of freedom.

Finally, the predominant loss of D_2O from $DOCH_2CH_2NDOD^{\bullet+}$, see inset of Fig. 3a, is readily explained by the proposed mechanism, as is the fate of the label: evidence that the N–H of ion **3**a is labelled is provided by the shift of the m/z 28 and 29 peaks in Fig. 3c to m/z 29 and 30 in Fig. 3d. Likewise, the isotopologue $HOCH_2CD_2NHOH^{\bullet+}$ specifically loses H_2O to yield m/z 61 ions whose CID mass spectrum displays prominent peaks at m/z 29 ($DC{=}NH^+$) and m/z 31 ($CD_2{=}NH^{\bullet+}$), see Fig. 3e.

Thus, we propose that 1,2-oxazetidine ions **3**a are generated via the mechanism proposed in Scheme 3.

3.4. Alternative pathways for the loss of H_2O from $HOCH_2CH_2NHOH^{\bullet+}$

To back up the above proposal we have performed a great many exploratory calculations of other pathways for the loss of water from metastable ions **HE**1. The most relevant of these are summarized in Scheme 6.

An a priori alternative route to the formation of 1,2-oxazetidine ions **3**a involves the O–H–N bridged conformer **HE**1d, which communicates with **HE**1a via a double rotation. A 1,4-H shift in **HE**1d yields **HE**5a and **HE**5b, energetically equivalent rotamers of a distonic ion. Of these, **HE**5b may ring-close to **HBRC**6. The H_2O molecule therein acts as an efficient catalyst for the reaction **HBRC**6 → **HBRC**3a → **3**a + H_2O, but the energy barrier for the prerequisite ring-closure is too great (179 kcal mol^{-1}). Considering the overall energy requirement (170 kcal mol^{-1}), ring-closure of **HE**5a to the three-membered species **HBRC**5 may also be discounted.

Scheme 6 also displays two routes involving a 1,3-H shift of a methylene H of the CH_2NH moiety of **HE**1. These are **HE**1a → **HE**1d → **HBRC**7 → **7**a + H_2O and **HE**1a → **HE**8 → **8** + H_2O. The TS for the 1,3-H shift associated with the first pathway (177 kcal mol^{-1}) is prohibitively high and the same undoubtedly obtains for the conversion **HE**1a → **HE**8, whose TS we could not

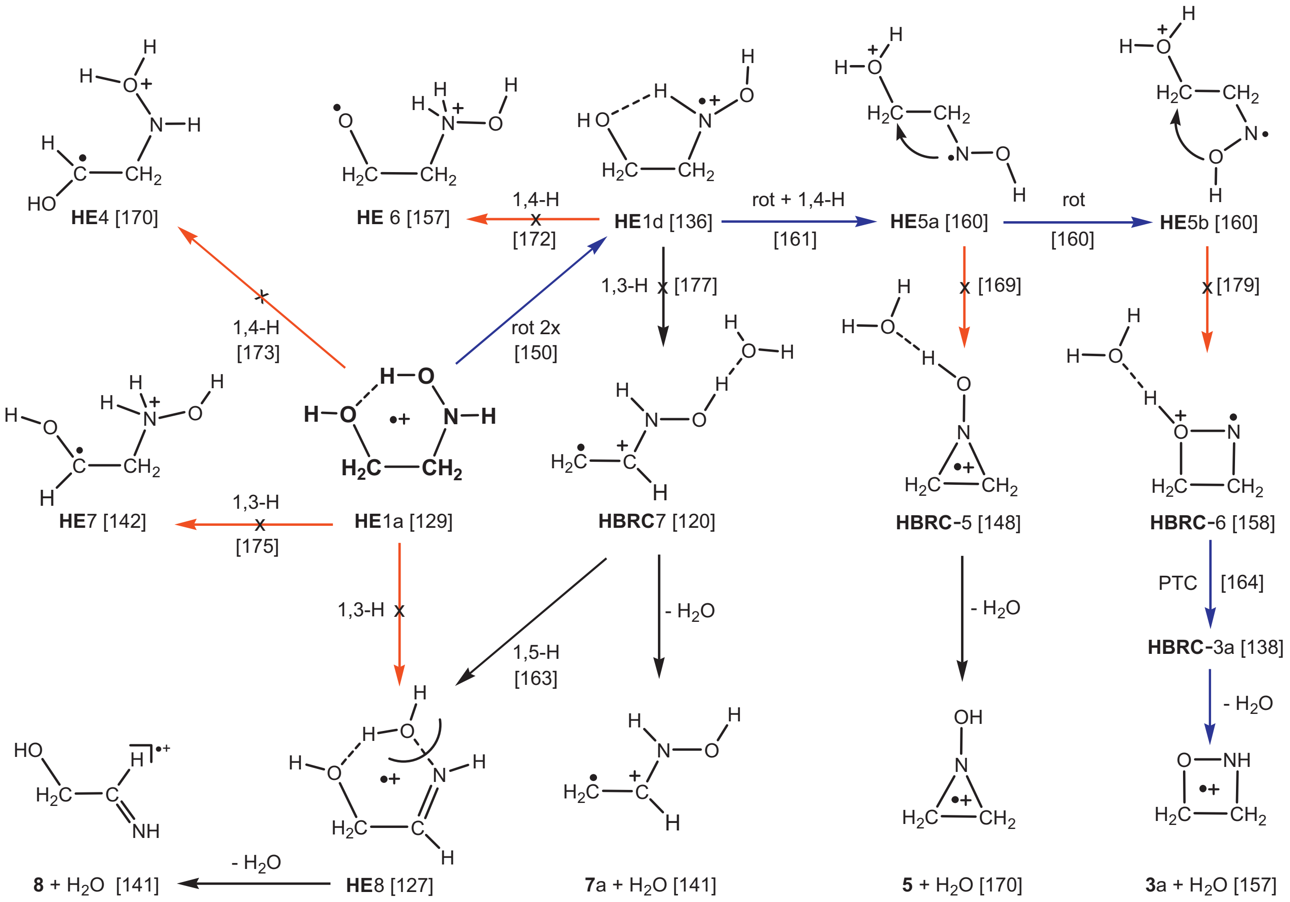

Scheme 6.

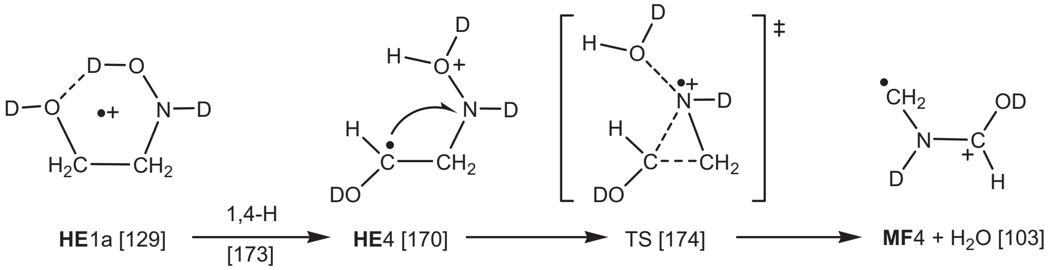

Scheme 7.

locate. The observation that $HOCH_2CD_2NHOH^{\bullet+}$ loses H_2O only, shows that these two 1,3-H shifts do not occur.

The third 1,3-H shift depicted in Scheme 6, **HE**1a → **HE**7, involves a methylene H of the CH_2OH moiety of **HE**1. This 1,3-H shift has a high barrier at 175 kcal mol^{-1} whereas the corresponding 1,4-H shift **HE**1a → **HE**4 lies at 173 kcal mol^{-1}. The direct bond cleavage **HE**1 → CH_2NHOH^+ (m/z 46) lies at 171 kcal mol^{-1}, so that these processes are not expected to play an important role in the dissociation chemistry of the metastable ions **HE**1. However, the conversion **HE**1 → **HE**4 could account for the minor loss of HDO (∼5%) observed in the MI and CID mass spectra of $DOCH_2CH_2NDOD^{\bullet+}$, see Fig. 3a and b. As shown in Scheme 7, ions **HE**4 need only 4 kcal mol^{-1} of internal energy to lose HDO to generate N–D labelled ions **MF**4. A collision experiment on the m/z 61 ions could confirm the putative structure of ions **MF**4, but unfortunately the signal intensity was not sufficient to obtain a meaningful CID mass spectrum.

It is conceivable that the above 1,3-H and 1,4-H shifts play a role in the water loss from **HE**1 ions that dissociate in the ion source. Their CID mass spectra (not shown) display a prominent cluster of peaks at m/z 24–34, whose intensity distribution is close to that of the metastable ions of Fig. 3c. The spectra also display a peak of comparable intensity at m/z 41, which could be attributed to the loss of H_2O from the $C_2H_5NO^{\bullet+}$ isomers **7** or **8**. This proposal remains highly speculative because the relative intensity of the m/z 41 peak in the CID spectra appeared to vary by more than a factor of two during the evaporation of the samples, indicating that part of the source-generated m/z 59 ions originates from thermal decomposition products.

4. Summary

The results of our combined experimental and computational study leave little doubt that the loss of H_2O from metastable 2-hydroxyaminoethanol ions **HE**1 generates 1,2-oxazetidine ions **3**a. As discussed in Section 3.1, ion **3**a is readily compatible with the features of the CID mass spectrum of Fig. 3c: the ion is characterized by a C–C atom connectivity and a $CH_2{=}NH$ structure motif represented by the cluster of peaks at m/z 24–29. Further, our calculations indicate that the generation of m/z 28 and 29 ions from **3**a is associated with a high reverse barrier in line with the observed kinetic energy release.

A mechanistic analysis using the CBS-QB3 model chemistry indicates that the dissociation of ions **HE**1 involves neither C–C bond cleavage (Section 3.2) nor 1,3-H or 1,4-H shift reactions (Section 3.4). Instead, see Section 3.3, theory predicts that the reaction is initiated by a 1,5-H transfer that leads to the formation of ionized 1,2-oxazetidine. The surprising efficiency of this reaction is readily explained by the substantial difference in adiabatic and vertical ionization energies: ions **HE**1 are generated with minimum internal energies close to the calculated critical energy of the proposed mechanism. Finally, the results of experiments with the isotopologues $DOCH_2CH_2NDOD^{\bullet+}$ and $HOCH_2CD_2NHOH^{\bullet+}$ fit nicely with the above proposal.

Acknowledgements

JKT and KJJ thank the Natural Sciences and Engineering Research Council of Canada (NSERC) for financial support. JKT and KJJ gratefully acknowledge valuable discussions with Dr. J.L. Holmes. Thanks are also due to Mr. T. Mahmood for preparing the sample of $HOCH_2CD_2NO_2$.

References

[1] V.Y. Taguchi, Rapid Commun. Mass Spectrom. 15 (2001) 455.
[2] K.J. Jobst, M.A. Trikoupis, V.Y. Taguchi, J.K. Terlouw, in preparation.
[3] K.J. Jobst, P.J.A. Ruttink, J.K. Terlouw, Int. J. Mass Spectrom. 269 (2008) 165.
[4] (a) P.J.A. Ruttink, P.C. Burgers, L.M. Fell, J.K. Terlouw, J. Phys. Chem. A 102 (1998) 176;
(b) Y. Li, T. Baer, J. Phys. Chem. A 106 (2002) 8658;
(c) J.L. Holmes, J.K. Terlouw, in: N.M.M. Nibbering (Ed.), Encyclopedia of Mass Spectrometry, vol. 4, Elsevier, Amsterdam, 2005, p. 287.
[5] R. Lee, P.J.A. Ruttink, P.C. Burgers, J.K. Terlouw, Int. J. Mass Spectrom. 255 (2006), 244 and references cited therein.
[6] (a) J.L. Holmes, C. Aubry, P.M. Mayer, Assigning Structures to Ions in Mass Spectrometry, CRC Press, Boca Raton, 2007;
(b) Yu-Ran Luo, Handbook of Dissociation Energies in Organic Compounds, CRC Press, Boca Raton, 2003;
(c) NIST Chemistry WebBook, NIST Standard Reference Data Base Number 69, National Institute of Standards and Technology, Gaithersburg, MD, August 2007.
[7] G.A. McGibbon, P.C. Burgers, J.K. Terlouw, Int. J. Mass Spectrom. 136 (1994) 191.
[8] M.A. Trikoupis, P.C. Burgers, P.J.A. Ruttink, J.K. Terlouw, Int. J. Mass Spectrom. 217 (2002) 97.
[9] R. Lee, P.J.A. Ruttink, P.C. Burgers, J.K. Terlouw, Can. J. Chem. 83 (2005) 1847.
[10] P.C. Burgers, J.K. Terlouw, in: N.M.M. Nibbering (Ed.), Encyclopedia of Mass Spectrometry, vol. 4, Elsevier, Amsterdam, 2005, p. 173.
[11] (a) D.H. Magers, S.R. Davis, J. Mol. Struct. (Theochem.) 487 (1999) 205;
(b) A.L. Schwan, J. Warkentin, in: A.R. Katritzky, C.W. Rees, E.F.V. Scriven (Eds.), Comprehensive Heterocyclic Chemistry II, vol. 1b, Pergamon Press, Oxford, 1996, p. 969.
[12] H.F. van Garderen, P.J.A. Ruttink, P.C. Burgers, G.A. McGibbon, J.K. Terlouw, Int. J. Mass Spectrom. Ion Proc. 121 (1992) 159.
[13] L.M. Fell, J.T. Francis, J.L. Holmes, J.K. Terlouw, Int. J. Mass Spectrom. Ion Proc. 165/166 (1997) 179.
[14] (a) N.R. Ayyangar, K.C. Brahme, U.R. Kalkote, K.V. Srinivasan, Synthesis 11 (1984) 938;
(b) S. Ozaki, S. Nishiguchi, M. Masui, Chem. Pharm. Bull. 32 (1984) 2609;
(c) H.K. Kim, R.E. Bambury, H.K. Yaktin, J. Med. Chem. 14 (1971) 301;
(d) R. Borch, M.D. Bernstein, H.D. Durst, J. Am. Chem. Soc. 93 (1971) 2897;
(e) S. Andrew, J.S. Mendoza, Tetrahedron. Lett. 32 (1991) 1699.
[15] J.A. Montgomery Jr., M.J. Frisch, J.W. Ochterski, G.A. Petersson, J. Chem. Phys. 112 (2000) 6532.
[16] J.W. Ochterski, G.A. Petersson, J.A. Montgomery Jr., J. Chem. Phys. 104 (1996) 2598.
[17] M.J. Frisch, G.W. Trucks, H.B. Schlegel, G.E. Scuseria, M.A. Robb, J.R. Cheeseman, G. Scalmani, V. Barone, B. Mennucci, G.A. Petersson, H. Nakatsuji, M. Caricato, X. Li, H.P. Hratchian, A.F. Izmaylov, J. Bloino, G. Zheng, J.L. Sonnenberg, M. Hada, M. Ehara, K. Toyota, R. Fukuda, J. Hasegawa, M. Ishida, T. Nakajima, Y. Honda, O. Kitao, H. Nakai, T. Vreven, J.A. Montgomery Jr., J.E. Peralta, F. Ogliaro, M. Bearpark, J.J. Heyd, E. Brothers, K.N. Kudin, V.N. Staroverov, T. Keith, R. Kobayashi, J. Normand, K. Raghavachari, A. Rendell, J.C. Burant, S.S. Iyengar, J. Tomasi, M. Cossi, N. Rega, J.M. Millam, M. Klene, J.E. Knox, J.B. Cross, V. Bakken, C. Adamo, J. Jaramillo, R. Gomperts, R.E. Stratmann, O. Yazyev, A.J. Austin, R. Cammi, C. Pomelli, J.W. Ochterski, R.L. Martin, K. Morokuma, V.G. Zakrzewski,

G.A. Voth, P. Salvador, J.J. Dannenberg, S. Dapprich, A.D. Daniels, O. Farkas, J.B. Foresman, J.V. Ortiz, J. Cioslowski, Gaussian 09 (Revision A.02), Gaussian, Inc., Wallingford, CT, 2009.

[18] (a) G. van der Rest, L.B. Jensen, S. Abdel Azeim, P. Mourgues, H.E. Audier, J. Am. Soc. Mass Spectrom. 15 (2004) 966;
(b) G. van der Rest, J. Chamot-Rooke, P. Morgues, T.B. McMahon, H.E. Audier, J. Am. Soc. Mass Spectrom. 15 (2004) 966.

[19] (a) P.M.W. Gill, L. Radom, J. Am. Chem. Soc. 110 (1988) 4931;
(b) S. Humbel, I. Côte, N. Hoffmann, J. Bouquant, J. Am. Chem. Soc. 121 (1999) 5507.